Porous implants as drug delivery vehicles to augment host tissue integration

Paul A. Clark,* Eduardo K. Moioli,‡ D. Rick Sumner,† and Jeremy J. Mao‡,1

*Department of Neurological Surgery, University of Wisconsin–Madison, Madison, Wisconsin, USA; †Department of Anatomy and Cell Biology, Rush University, Chicago, Illinois, USA; and ‡Columbia University, College of Dental Medicine, Fu Foundation School of Engineering and Applied Sciences, Department of Biomedical Engineering, New York, New York, USA

ABSTRACT   The common premise of synthetic implants in the restoration of diseased tissues and organs is to use inert and solid materials. Here, a porous titanium implant was fabricated for the delivery of microencapsulated bioactive cues. Control-released transforming growth factor-β1 (TGF-β1) promoted the proliferation and migration of human mesenchymal stem cells into porous implants *in vitro*. At 4 wk of implantation in the rabbit humerus, control-released TGF-β1 from porous implants significantly increased bone-to-implant contact (BIC) by 96% and bone ingrowth by 50% over placebos. Control-released 100 ng TGF-β1 induced equivalent BIC and bone ingrowth to adsorbed 1 μg TGF-β1, suggesting that controlled release is effective at 10-fold less drug dose than adsorption. Histomorphometry, scanning electron microscopy, and microcomputed tomography showed that control-released TGF-β1 enhanced bone ingrowth in the implant's pores and surface. These findings suggest that solid prostheses can be transformed into porous implants to serve as drug delivery carriers, from which control-released bioactive cues augment host tissue integration.—Clark, P. A., Moioli, E. K., Sumner, D. R., Mao, J. J. Porous implants as drug delivery vehicles to augment host tissue integration. *FASEB J.* 22, 000–000 (2008)

Key Words: stem cells · transforming growth factor-β, bone morphogenetic proteins · osteoblasts · wound healing · controlled release

TISSUE AND ORGAN DEFECTS resulting from trauma, chronic diseases, tumor resection, or congenital anomalies necessitate the restoration of the lost anatomical structures. In comparison with donor site morbidity and pain in association with autologous tissue grafting, synthetic materials have the advantage of ready and endless supply without any sacrifice of donor tissue. During the past decades, the premise of the design of synthetic tissue implants has been to use inert and bulk materials that permit the integration of host tissue. Although this premise has been translated into a number of successful tissue replacement devices, such as cardiac stents, total joint prostheses, and dental implants, several limitations have become apparent such

as short implant life span and a lack of remodeling with host tissue. Aseptic "loosening" is the most common cause for implant failure (1, 2). Synthetic implants are subjected to wear and tear and do not remodel with host tissue such as cardiac muscle or bone (1, 2). There is often a mismatch of mechanical properties between synthetic implants and host tissue. For example, titanium (Ti) is ~10× stiffer than cortical bone and 100× stiffer than cancellous bone (3, 4). This disparity in mechanical stiffness between Ti and host bone creates stress shielding by diverting functioning mechanical stress, necessary for the health of peri-implant bone, to the Ti implant. Stress shielding leads to osteoclastogenesis and osteolysis (5–7). Another undesirable, and yet tolerated, feature of synthetic implants is the length of rehabilitation following surgery. Lengthy postsurgical rehabilitation is sometimes needed for orthopedic implants. For dental implants, several months of bone healing are currently required after implant placement prior to functional connection of dental prosthesis (1, 2). When implants fail, revision surgeries are costly and technically challenging. Thus, strategies that enhance tissue ingrowth and long-term biofixation are critically needed.

Several approaches have been devised to improve tissue ingrowth to synthetic implants. Surface modification is the most prevalent approach by changing surface topography or adsorbing bioactive factors. Certain topographic features fabricated on implant surface are generally associated with enhanced cell adhesion, such as osteoblast adhesion to implant surface (8–10). Bioactive cues are typically adsorbed to biomaterials, such as hydroxyapatite or hydrogel polymers, that are coated on the implant's surface. The transforming growth factor β (TGF-β) superfamily has been the most commonly used bioactive cues, including TGF-βs and bone morphogenetic proteins (BMPs) (11, 12). TGF-β1 plays a major role in the modulation of the behavior of multiple cell lineages, such as fibroblasts and osteoblasts, which are of relevance to wound healing and

tissue regeneration (12, 13). TGF-β1 also up-regulates molecules that are critical to tissue integration on implant surface and bone ingrowth, such as alkaline phosphatase, type I collagen, bone sialoprotein, and osteocalcin (14). TGF-β1 is further efficacious in increasing the calcium content and the size of calcified nodules of primary osteoblasts (14). BMP2 immersed in calcium phosphate-coated Ti implants yields ~50% more bone ingrowth (15). When adsorbed directly on Ti surface, BMP2 is not osteogenic, but BMP2 adsorbed in calcium phosphate coating on Ti surface induces bone ingrowth (16). Similarly, BMP7/OP1 adsorbed in periapatite-coated Ti implant increases bone ingrowth by ~65% (17). However, a critical drawback in the common approach of growth factor adsorption is premature denature and diffusion of the delivered proteins or peptides, usually within minutes of exposure to *in vivo* enzymes and catalysts (18–20). Although the efficacy of cytokines adsorbed in implant-coating materials has been reported in animal models, higher cytokine doses are likely needed in humans, leading to high cost, potential toxicity, and other obstacles in the regulatory process.

A control release system overcomes the limitation of rapid denature and diffusion of growth factors *in vivo*, thus potentially reducing drug dose. An effective controlled-release system is to encapsulate bioactive cues in biocompatible and biodegradable microparticles (18–20). As microparticles undergo degradation, biological cues are released with predesigned dose kinetics over time. We recently showed that microparticle-encapsulated and control-released TGF-β3 at up to 1 ng/ml inhibits the osteogenic differentiation of bone marrow-derived human mesenchymal stem cells (hMSC) and the elaboration of an osteogenic matrix (19, 21), presenting potential applications in wound healing, including the inhibition of ectopic bone formation. Although previous work has meritoriously focused on the adhesion and proliferation of osteoblasts on implant surface, little is known about the roles played by mesenchymal stem cells (MSC), the progenitors of osteoblasts, in implant wound healing. The recruitment and proliferation of MSC will enrich the populations of osteoprogenitors and osteoblasts and are likely critical to the initial stage of implant wound healing (19, 21). In this report, we designed and fabricated a porous Ti implant as a drug carrier for the delivery of microencapsulated TGF-β1 and showed that control-released TGF-β1 not only increased the proliferation of hMSC, but also hMSC migration, in a gelatin sponge inserted into a porous titanium implant. Control-released TGF-β1 from the porous Ti implant *in vivo* augmented bone-to-implant contact and bone ingrowth in both the surface and pores of Ti implant, providing the possibility of bone formation from inside out by hMSC that have already migrated into the implant pores. Collectively, these findings suggest the transformation of solid synthetic prostheses into porous implants as a drug delivery carrier for the delivery of bioactive cues to augment tissue ingrowth.

MATERIALS AND METHODS

Microencapsulation of TGF-β1

Microencapsulation of TGF-β1 in polylactic-coglycolic acid (PLGA) (**Fig. 1A**) was achieved using a double emulsion technique [(water-in-oil)-in-water] (19). PLGA is degraded by hydrolysis into biocompatible byproducts, including lactic and glycolic acid monomers. Lactic and glycolic acids are eliminated *in vivo* as CO_2 and H_2O *via* the Krebs cycle, eliciting minimal adverse response (22). Recombinant human TGF-β1 with a molecular weight of 25 kDa (R&D Systems, Minneapolis, MN, USA) was reconstituted in 1% BSA solution. A 50-μl solution containing either 250 ng of TGF-β1 (low dose as in Fig. 1B), 2.5 μg of TGF-β1 (high dose as in Fig. 1C), or PBS (placebo control) was added to a 25% w/v PLGA solution (Sigma, St. Louis, MO, USA) that was dissolved in dichloromethane (250 mg PLGA:1 ml dichloromethane). This primary emulsion was vortexed and stabilized in 1% polyvinyl alcohol (PVA, 30,000–70,000 MW, Sigma, St. Louis, MO, USA) [(water-in-oil)-in-water]. The resulting mixture was added to 100 ml of 0.1% PVA solution for 1 min, followed by the addition of 100 ml of 2% isopropanol, and was stirred under a fume hood for 2 h at 400–500 rpm to allow for vaporization of the solvent (dichloromethane). The microparticles (MPs) were collected by filtration through a 2-μm filter. MPs were observed using a light microscope, with their average diameter measured by fitting circles to match randomly selected MPs. The MPs were frozen in liquid nitrogen, lyophilized (19, 22), and stored at −20°C. Placebo MPs encapsulating PBS were used as controls to determine any potential effects of PLGA degradation byproducts (19). Initial encapsulation efficiency was determined by dissolving 10 mg of TGF-β1-encapsulated MPs in dichloromethane, adding 1% BSA, and allowing the solution to separate overnight. The released TGF-β1 from MPs was quantified from the aqueous phase using an ELISA, with its encapsulation efficiency calculated as described previously (22).

TGF-β1 release kinetics

The release kinetics of TGF-β1 from the PLGA MPs was determined and used to calculate dosing in subsequent studies (Fig. 1B, C). MPs were suspended in 1% BSA and set in a water bath at 37°C shaking at 60 rpm. At defined time points, MPs were centrifuged at 5000 rpm, followed by the collection of supernatant. The PLGA MPs were then resuspended in 1% BSA and placed back in water bath. The total amount of TGF-β1 in each supernatant sample was quantified using ELISA to construct release kinetics (19, 22).

Isolation of human mesenchymal stem cells

Fresh bone marrow samples of multiple adult male donors (AllCells, Berkeley, CA, USA) were used to isolate MSC, per our previous methods (19, 23). Nonadherent cells were removed by negative selection (19, 23). Human MSCs were purified by centrifugation through a density gradient (Ficoll-Paque, StemCell Technologies, Seattle, WA, USA) and using negative selection following manufacturer's protocol (RosetteSep, StemCell Technologies, Vancouver, BC, Canada) to remove hematopoietic and differentiated cells, identified by the cell surface markers Glycophorin A, CD3, CD14, CD19, CD66b, and CD38. The isolated mononuclear and adherent cells were counted under an inverted microscope, plated in basal medium (Dulbecco's modified Eagle's medium+10% fetal bovine serum+1% antibiotic-
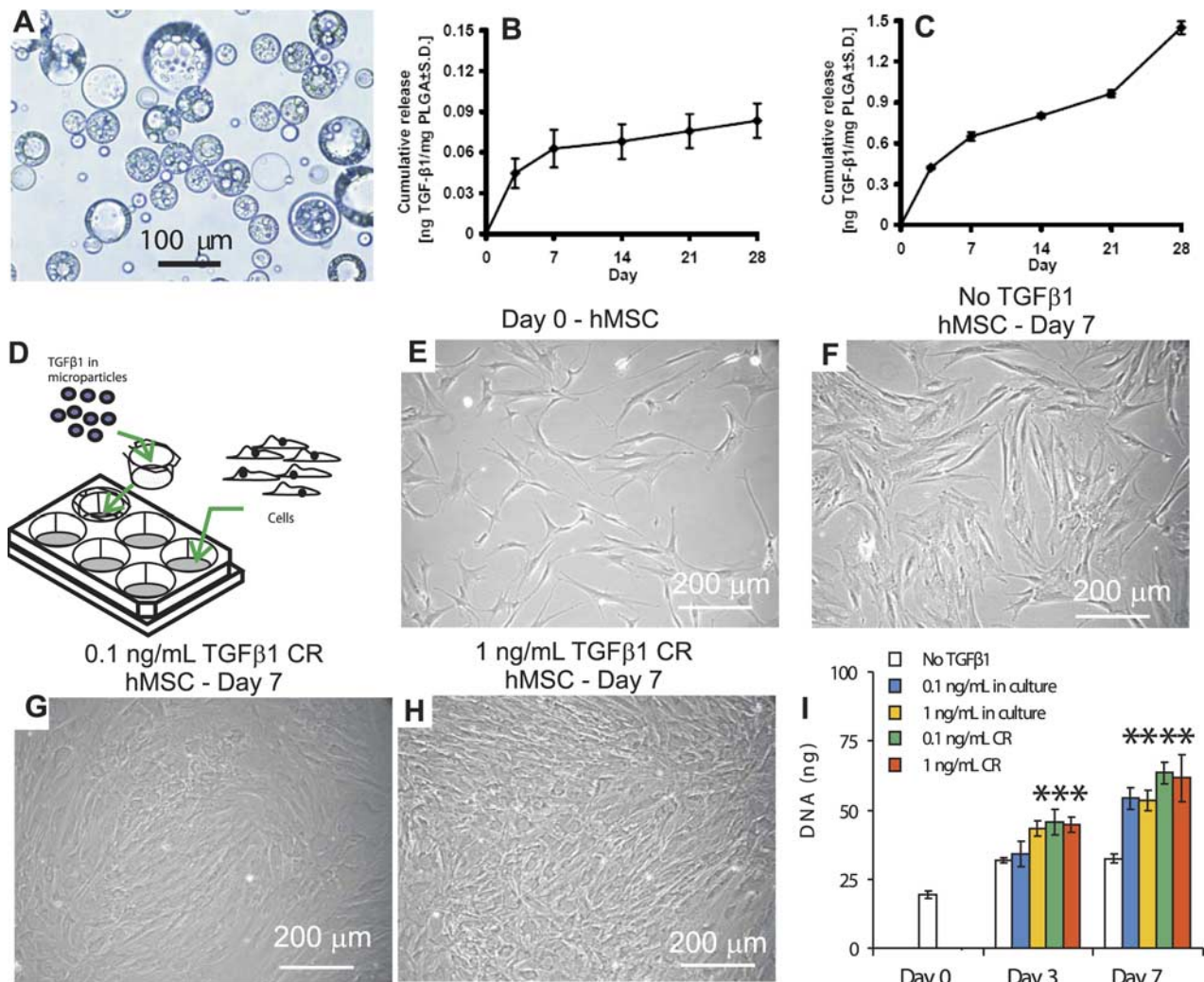
Figure 1. The effects of control-released TGF-β1 on the proliferation of human mesenchymal stem cells. PLGA microparticles (MPs) were fabricated to encapsulate TGF-β1 by double emulsion (*A*). The release kinetics of microencapsulated TGF-β1 was studied with a low dose of 250 ng (*B*) and a high dose of 2.5 μg (*C*). Despite the anticipated 10-fold higher release dose for 2.5 μg TGF-β1 than for 250 ng TGF-β1, similar release profiles between the low and high doses indicate the stability and versatility of the controlled release (CR) system. hMSCs were isolated from bone marrow of multiple adult donors and culture-expanded. TGF-β1-encapsulating or placebo MPs were placed in transwell inserts (*D*), which were submerged in the culture of underlying hMSC. Microscopically, marked hMSC proliferation at day 7 was observed on the treatment of control-released TGF-β1 at 0.1 ng/ml (*G*), and more markedly at 1 ng/ml (*H*), in comparison to day 0 (*E*) or no TGF-β1 delivery at day 7 (*F*). Control-released TGF-β1 at doses of 0.1 and 1 ng/ml significantly increased the DNA content of hMSC (*n*=6; *$P<0.05$, **$P<0.01$) at both 3 and 7 days, as compared to TGF-β1-free group (*I*). The DNA content of control-released 0.1 and 1 ng/ml TGF-β1 lacked significant differences from the DNA content of hMSC (*E*) treated with dose-matched TGF-β1 added to culture medium (without encapsulation), verifying the bioactivity of control-released TGF-β1. Importantly, the increased proliferation of hMSC by control-released TGF-β1 may have implications in the initial phase of implant wound healing.

antimycotic) at ~0.5–1 × 10^6 cells per 100-mm petri dish, and incubated at 37°C and 5% CO_2. After 24 h, nonadherent cells were discarded, whereas adherent cells were washed twice with PBS and incubated for 12 days with fresh medium change every 3 to 4 days. The remaining mononuclear and adherent cells consist of heterogeneous cell lineages, including fibroblasts, osteoprogenitors, and MSC (23). We and others have previously shown that this heterogeneous cell population of bone marrow-derived, mononucleated cells contains MSC that can proliferate to a number of passages, and then differentiate into osteoblasts, chondrocytes, adipocytes, *etc.* (23). On 80 to 90% confluence, primary MSC were trypsinized and passaged, approximately every 7 days.

Cell proliferation assay

PLGA MPs were sterilized by ethylene oxide (EO), which does not significantly affect the release profile (19). The release profile of TGF-β1 showed the release of 0.06 ng/mg TGF-β1 after 7 days culturing with 5 or 50 mg of MPs and 3 ml of growth medium, a solution concentration of 0.1 or 1 ng/ml, respectively, of TGF-β1. Either 5 or 50 mg of MPs (low density), corresponding to 0.1 or 1 ng/ml of TGF-β1 released after 7 days, respectively, was placed in a transwell insert with a 0.4-μm diameter porous membrane (Fig. 1*D*). Transwell inserts allowed MPs to be suspended 0.9 mm above a monolayer of hMSC, while the pores allowed passage of TGF-β1 released from the PLGA MPs (19) (Fig. 1*D*). Five milligrams

of MPs encapsulating PBS were used as placebo controls. For hMSC exposed to TGF-β1 in solution, the TGF-β1 was diluted to the desired concentration in corresponding medium and replenished every media change. The transwell inserts containing PLGA MPs were placed into the 6-well dishes over the monolayers of hMSC and cultured for 0, 3, and 7 days (Fig. 1E–H). Medium was changed at day 5 to maximize the bioactivity of control-released TGF-β1 from PLGA MPs. At each time point, corresponding monolayers of cells were submersed in 0.5 ml of 1% Triton-X for 20 min, collected using a cell scraper, and homogenized using sonication to form a cell lysate. Total DNA content of the cell lysate was determined using Hoechst 33258 dye (Fluorescent DNA Quant. Kit; Bio-Rad; Hercules, CA, USA), per our prior methods (19) (Fig. 1I). The bioactivity of control-released TGF-β1 was tested using a proliferation assay (19). Various concentrations of control-released TGF-β1 were compared with dose-corresponding TGF-β1 added in cell culture (without microencapsulation) (Fig. 1I).

Three-dimensional *in vitro* cell migration model

A hollow Ti implant module (7×6 mm; length×diameter) was fabricated and sterilized by autoclave (**Fig. 2A**). A gelatin sponge (Gelfoam, Pharmacia, Kalamazoo, MI, USA) with pore sizes of 200–500 μm was chosen as a carrier for PLGA MPs, given its previously demonstrated support of hMSC growth and wide use in bone regeneration (24). Scanning electron microscopy (SEM) (S-3000N; Hitachi, Tokyo, Japan) confirmed the pore size range of 200–500 μm. MPs encapsulating TGF-β1 or PBS (placebo control) were infused into the gelatin sponge by negative pressure, which was inserted in the hollow core of the Ti implant (Fig. 2A). The hollow Ti implant was placed onto a monolayer of hMSC (Fig. 2A). The following TGF-β1 doses and delivery modes were investigated: 5 mg of low-density TGF-β1 MPs (≈0.1 ng/ml TGF-β1), 5 mg of high-density TGF-β1 MPs (≈1 ng/ml TGF-β1), or 5 mg of placebo MPs encapsulating PBS. Cell culture was incubated with fresh medium changes every 5 days. At predesignated 7, 14, and 28 days, gelatin sponges from inside the Ti implants were removed and rinsed. Cell metabolic activities to assess cell number were determined using a colorimetric assay with a tetrazolium compound [3-(4,5-dimethylthiazol-2-yl)-5-(3-carboxymethoxyphenyl)-2-(4-sulfophenyl)-2H-tetrazolium, inner salt; MTS] following the manufacturer's protocol (Cell-Titer 96 AQueous One Solution Cell Proliferation Assay, Promega, Madison, WI, USA) and per our prior methods (19). The MTS compound is reduced by viable cells into a formazan product measurable by 490 nm absorbance, presumably accomplished by NADPH or NADH produced by dehydrogenase enzymes in metabolically active cells, and can also function as an indirect measure of cell proliferation or number (25). The MTS solution was diluted 1:10 in serum-free DMEM without phenol red. Each gelatin sponge was completely immersed in MTS and incubated for 1 h, followed by the collection of the supernatant and reading on a microplate reader at 490 nm. At each time point, all samples were normalized to the placebo MP group without TGF-β1. Cell migration was visualized by fluorescent nuclear staining using 4′, 6-diamidino-2-phenylindole, dihydrocholoride (DAPI) (Sigma-Aldrich, St. Louis, MO, USA) and observed in PBS under fluorescence (Leica DMIRB, Leica Microsystems, Bannockburn, IL, USA) with appropriate filters.
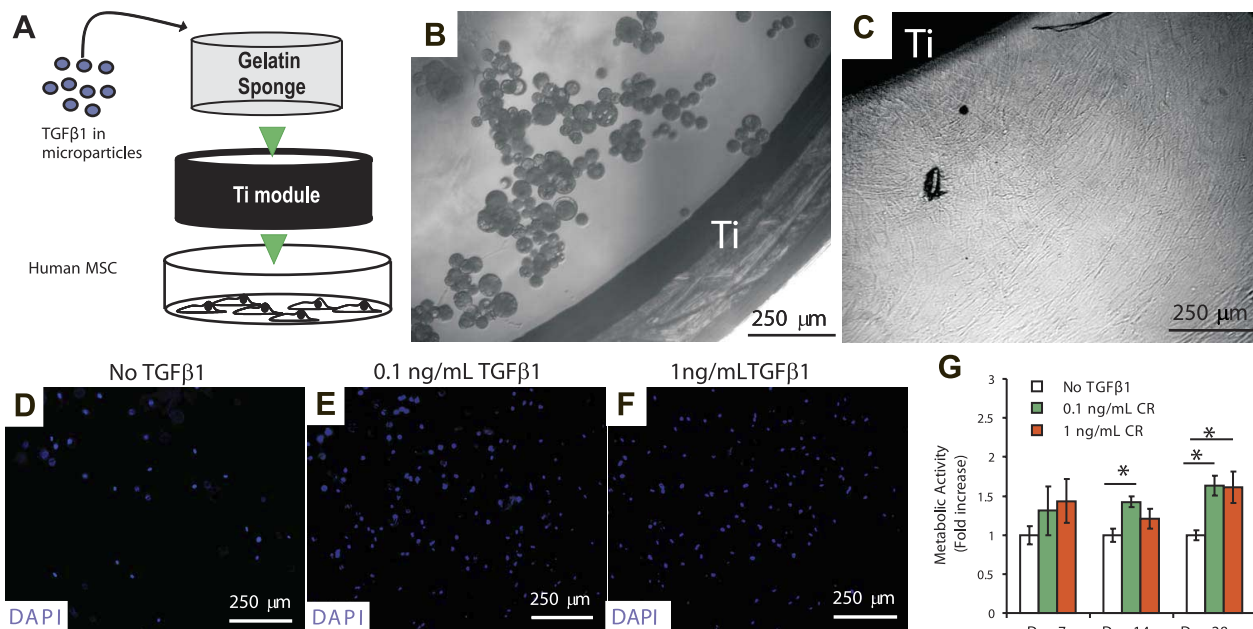

Figure 2. Control-released TGF-β1 from the porous Ti implant induces the migration of hMSC. Microencapsulated TGF-β1 was infused into gelatin sponge that was placed into the hollow core of a custom-made Ti implant (*A*). The porous Ti implant was submerged in the culture of hMSCs (*A*). MPs encapsulating TGF-β1 remained in the gelatin sponge within the porous Ti implant at day 28 (*B*). Abundant hMSC were present next to the outer wall of the Ti implant in response to 1 ng/ml control-released (CR) TGF-β1 at 28 days (*C*). Fluorescent nuclear staining, DAPI, of the gelatin sponges infused with microencapsulated 0.1 ng/ml (*E*) or 1 ng/ml (*F*) TGF-β1 showed abundant hMSC that had migrated into the porous Ti implant from underlying culture against gravity, in comparison with TGF-β1-free sample (*D*). Control-released TGF-β1 at both 0.1 and 1 ng/ml significantly increased the metabolic activity of hMSC, an indirect measure of cell proliferation and number, at 14 and 28 days, in comparison with TGF-β1-free group (*G*) (n=6; *$P<0.05$).

In vivo implantation of porous titanium implants

All animal procedures were approved by the local Institutional Animal Care and Use Committee. Commercially pure Ti was cast into porous cylinder module implants with dimensions of 2.8×4 mm (diameter×length), a hollow inner core (1.8 mm in diameter) and pores on the Ti wall (0.8 mm in diameter) for *in vivo* implantation. A gelatin sponge was inserted into the hollow core of Ti implant and contained the following TGF-β1 doses: 5 mg high-density TGF-β1 MPs (≈100 ng) infused by negative pressure, adsorption of 100 ng or 1 μg TGF-β1 in gelatin sponges by overnight soaking (26), or 5 mg placebo MPs encapsulating PBS. The porous Ti implants were surgically implanted into the humeri of skeletally mature New Zealand White rabbits (3.5–4.0 kg) using aseptic technique under general anesthesia, similar to our previous approach (19). The rabbit proximal humerus was chosen instead of more traditional models such as the tibia or femur (27, 28) because of low incidence of bone fracture of the humerus. An incision of ~3 cm was made in the shoulder region, with the subcutaneous soft tissue deflected, and the periosteum was stripped using a periosteal elevator. Using a rotary handpiece (Straumann, Andover, MA, USA) at no more than 1000 rpm, we drilled pilot holes of increasing diameter (2.2–2.8 mm) unicortically into the medullary cavity. Ti implants were line-to-line fit, followed by wound closure. The same procedure was then repeated on the contralateral side for the placement of identical implants, given that growth factors delivered in one limb may affect the contralateral limb (29). Animals were allowed normal cage activity during the entire healing process. Calcein blue (30 mg/kg) was injected subcutaneously at 3 wk to label newly formed bone (30).

Tissue harvesting, preparation and analysis

At 4 wk postsurgery, implant samples were removed with surrounding bone *en bloc* and embedded in methyl methacrylate. Samples were trimmed using a diamond saw and polished using diamond paper to 5 μm on a grinder/polisher system (Trizact, 3M, St. Paul, MN, USA). For secondary ion scanning electron microscopy, samples were sputter coated with platinum/palladium (Pt/Pd) metal films of ~3 nm and imaged under high voltage and constant pressure (Hitachi S-3000N Variable Pressure-SEM). Bone-to-implant contact (BIC) and bone volume to tissue volume (BV/TV) within 0.8 mm pores of the porous Ti implants were quantified using computerized image analysis software (30) (ImagePro Plus, Media Cybernetics, Silver Spring, MD, USA). Microcomputed tomography (μCT) (Scanco 40; Scanco, Wayne, PA, USA) was used to scan bone-implant samples at intervals that correspond to a resolution of ≈20 μm in plane and slice thickness of ≈20 μm (31). For histology, samples were glued to plastic slides, ground to thin sections using diamond paper, and stained using hematoxylin and eosin (H&E), per our prior approach (30).

Data analysis and statistics

A one-way ANOVA with *post hoc* Bonferroni tests was performed to determine any significant differences between or within all groups in which numerical data were generated using at an α level of $P < 0.05$.

RESULTS

Dose-independent release kinetics of microencapsulated TGF-β1

A sample of PLGA MPs fabricated by double emulsion is shown under light microscopy, with an average diameter of 64 ± 16 μm (Fig. 1A), which can be fine-tuned for yielding different release kinetics. To determine whether the initial encapsulation dose affects release kinetics, we compared a low dose of 250 ng TGF-β1 (Fig. 1B) and a high dose of 2.5 μg TGF-β1 (Fig. 1C), both encapsulated in 250 mg PLGA. The release profiles were similar regardless of the initial TGF-β1 encapsulation amount (Fig. 1B, C), suggesting the stability and versatility of the present drug delivery system. For both low and high TGF-β1 doses, an initial burst release at day 3 was sustained up to the tested 4 wk (Fig. 1B, C), consistent with previous demonstration of control-released growth factors *in vitro* up to several months (19, 21). As anticipated, a 10-fold higher release dose was observed with 2.5 μg TGF-β1 (Fig. 1C) than with 250 ng TGF-β1 (Fig. 1B), further indicating the efficacy of the drug delivery system.

Control-released TGF-β1 induces the proliferation of human mesenchymal stem cells in monolayer culture

Fresh bone marrow samples of multiple adult male donors were prepared to isolate hMSC, per our previous approaches (19, 21, 23, 32). The effects of control-released TGF-β1 on the proliferation rates of hMSC were compared with dose-matched TGF-β1 added to culture medium (without microencapsulation). A submerged transwell system allowed the release of microencapsulated TGF-β1 into the underlying cells in culture medium, and yet without direct contact between MPs and cells (Fig. 1D). Microscopically, marked hMSC proliferation at day 7 was observed with control-released TGF-β1 at 0.1 ng/ml (Fig. 1G), and more markedly at 1 ng/ml (Fig. 1H), in comparison to day 0 (Fig. 1E) or no TGF-β1 delivery at day 7 (Fig. 1F). These qualitative observations of cell proliferation are substantiated quantitatively by DNA content of hMSC. When treated with control-released TGF-β1 at either 0.1 ng/ml ($n=6$, $P<0.01$) or 1 ng/ml ($n=6$, $P<0.01$ at day 3, $P<0.05$ at day 7), DNA content was significantly higher than placebo MPs at days 3 and 7 (Fig. 1I). Importantly, the DNA content of hMSC treated with control-released TGF-β1 at either 0.1 or 1 ng/ml showed no significant differences from that of dose-matched TGF-β1 added to culture medium (Fig. 1I), further indicating the efficacy of the controlled-release system.

Control-released TGF-β1 from hollow titanium implant is chemotactic to human mesenchymal stem cells

The hollow Ti implant with microencapsulated TGF-β1 or placebo MPs was placed in hMSC culture (Fig. 2A).

MPs were observed inside the hollow Ti implant up to the tested 28 days (Fig. 2B). Adjacent to the outer wall of the hollow Ti implant, abundant hMSC accumulated in response to control-released 1 ng/ml TGF-β1 at 28 days (Fig. 2C). DAPI nuclear staining visualized the number of hMSC that had migrated into the gelatin sponge from the underlying cell culture against gravity, indicating the chemotactic effects of control-released TGF-β1. By day 28, there were abundant hMSC in the gelatin sponges infused with microencapsulated TGF-β1 at either 0.1 ng/ml (Fig. 2E) or 1 ng/ml (Fig. 2F), although cell migration also occurred in the TGF-β1-free sample (Fig. 2D). The metabolic activity of hMSC, measured by cleavage of MTS tetrazolium compound by viable cells, that had migrated into the gelatin sponges was significantly higher at 14 days for control-released 0.1 ng/ml TGF-β1 ($n=6$, $P<0.05$), and at 28 days for either 0.1 or 1 ng/ml TGF-β1 ($n=6$, $P<0.05$) than TGF-β1-free group (Fig. 2G), suggesting that control-released TGF-β1 up-regulates the metabolic activity of the migrated hMSC. Increased metabolic activity of migrated hMSC also functioned as an indi-rect marker of cell number (25), supporting DAPI staining.

In vivo implantation of TGF-β1-encapsulated MPs in porous Ti implant

The porous Ti implants were implanted unicortically in the humerus bones of skeletally mature New Zealand White rabbits (**Fig. 3A–C**). Following 4 wk *in vivo* implantation, Ti implants were found firmly integrated with host bone by radiographic examination (Fig. 3D) and remained integrated after embedding in me-thymethacrylate and bisection of the Ti implant with a diamond knife (Fig. 3E). Interconnecting pores of the Ti implant are visible (Fig. 3E).

Control-released TGF-β1 from porous Ti implant significantly augments bone-to-implant contact and bone ingrowth *in vivo*

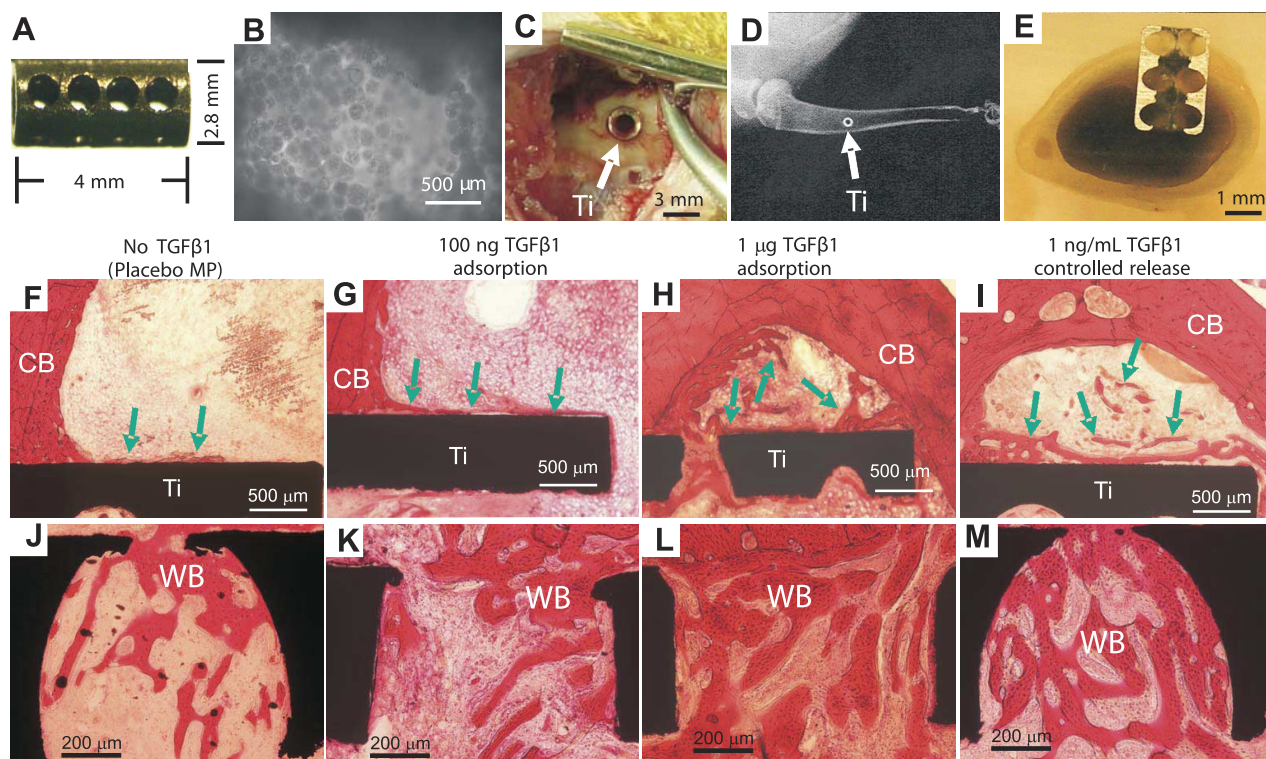In comparison to moderate bone-to-implant contact in the TGF-β1-free implant (placebo MPs) (Fig. 3F) or 100

Figure 3. *In vivo* bone ingrowth in porous Ti implants by TGF-β1 delivery. A porous Ti implant was custom-fabricated (*A*). MPs encapsulating TGF-β1 or placebo MPs (*B*) were infused into a gelatin sponge by negative pressure and placed into the porous Ti implant for *in vivo* implantation unicortically in the humerus of skeletally mature rabbit (*C*). Postoperative radiograph (*D*) and harvested implant-bone sample embedded in methymethacrylate (*E*) demonstrate the integration and unicortical placement of the porous Ti implant in the proximal humerus. After 4 wk *in vivo* implantation, bone-to-implant contact (BIC) is moderate in TGF-β1-free sample (placebo MPs) (*F*) or 100-ng gelatin-adsorbed TGF-β1 sample (*G*). In contrast, BIC for both 1-μg gelatin-adsorbed TGF-β1 implant (*H*) and 1 ng/ml control-released TGF-β1 implant (*I*) is substantial. The total amount of control-released 1 ng/ml TGF-β1 for the tested 4 wk of *in vivo* implantation is calculated to be ∼100 ng, since 19.11 ± 3.50 ng microencapsulated TGF-β1/mg TGF-β1 MPs × 5 mg implanted TGF-β1 MPs ≈ 100 ng TGF-β1. Thus, 1 ng/ml control-released TGF-β1 was equally effective to 1 μg gelatin-adsorbed TGF-β1, and yet at a 10-fold lower drug dose. Similarly, bone ingrowth in the pores of Ti implants for both 1 μg gelatin-adsorbed TGF-β1 (*L*) and 100 ng of MP-encapsulated TGF-β1 (*M*) is substantial, in comparison to sparse bone ingrowth in the pores of Ti implant without TGF-β1 (*J*) or with 100 ng of gelatin-adsorbed TGF-β1 (*K*). Hematoxylin-and-eosin (H&E) staining. CB, cortical bone; WB, woven bone.

ng/ml gelatin-adsorbed TGF-β1 implant (Fig. 3*G*), there was substantial BIC for both 1-μg gelatin-adsorbed TGF-β1 implant (Fig. 3*H*) and 1 ng/ml control-released TGF-β1 implant (Fig. 3*I*). The total amount of control-released 1 ng/ml TGF-β1 for the tested 4 wk of *in vivo* implantation is calculated to be 100 ng, since 19.11 ± 3.50 ng microencapsulated TGF-β1/mg TGF-β1 MPs × 5 mg implanted TGF-β1 MPs ≈ 100 ng TGF-β1. Thus, 1 ng/ml control-released TGF-β1 is as effective as 1 μg gelatin-adsorbed TGF-β1, but at a 10-fold lower drug dose. Similarly, both 1 μg gelatin-adsorbed TGF-β1 (Fig. 3*L*) and 1 ng/ml microencapsulated TGF-β1 (Fig. 3*M*) induced marked bone ingrowth in the pores of Ti implants, in comparison to moderate bone ingrowth without TGF-β1 (Fig. 3*J*) or with 100-ng gelatin-adsorbed TGF-β1 (Fig. 3*K*). These qualitative findings are substantiated below by SEM (Fig. 5*A–C*) and μCT imaging (Fig. 5*D–F*) of bone ingrowth, and further by quantitative, computerized histomorphometry of BIC and bone ingrowth (Fig. 5*G*).

Further examination reveals the ingrowth of substantial woven bone (WB) that was integrated with cortical bone (CB) for both 1-μg gelatin-adsorbed TGF-β1 implant (**Fig. 4***B*) and 1 ng/ml control-released TGF-β1 implant (Fig. 4*C*), in comparison to moderate WB formation in the TGF-β1-free implant (Fig. 4*A*). The newly formed WB was surrounded by bone marrow cavities (Fig. 4*D–F*), known as a source of osteoprogenitor cells and/or mesenchymal stem cells (23, 32). Calcein labeling revealed marked new bone formation for both 1-μg gelatin-adsorbed TGF-β1 implant (Fig. 4*H*) and 1 ng/ml microencapsulated TGF-β1 implant (Fig. 4*I*), in comparison to moderate new bone formation adjacent to the TGF-β1-free Ti implant (Fig. 4*G*).

SEM showed marked BIC and WB formation in the surface and pores of both 1 μg gelatin-adsorbed
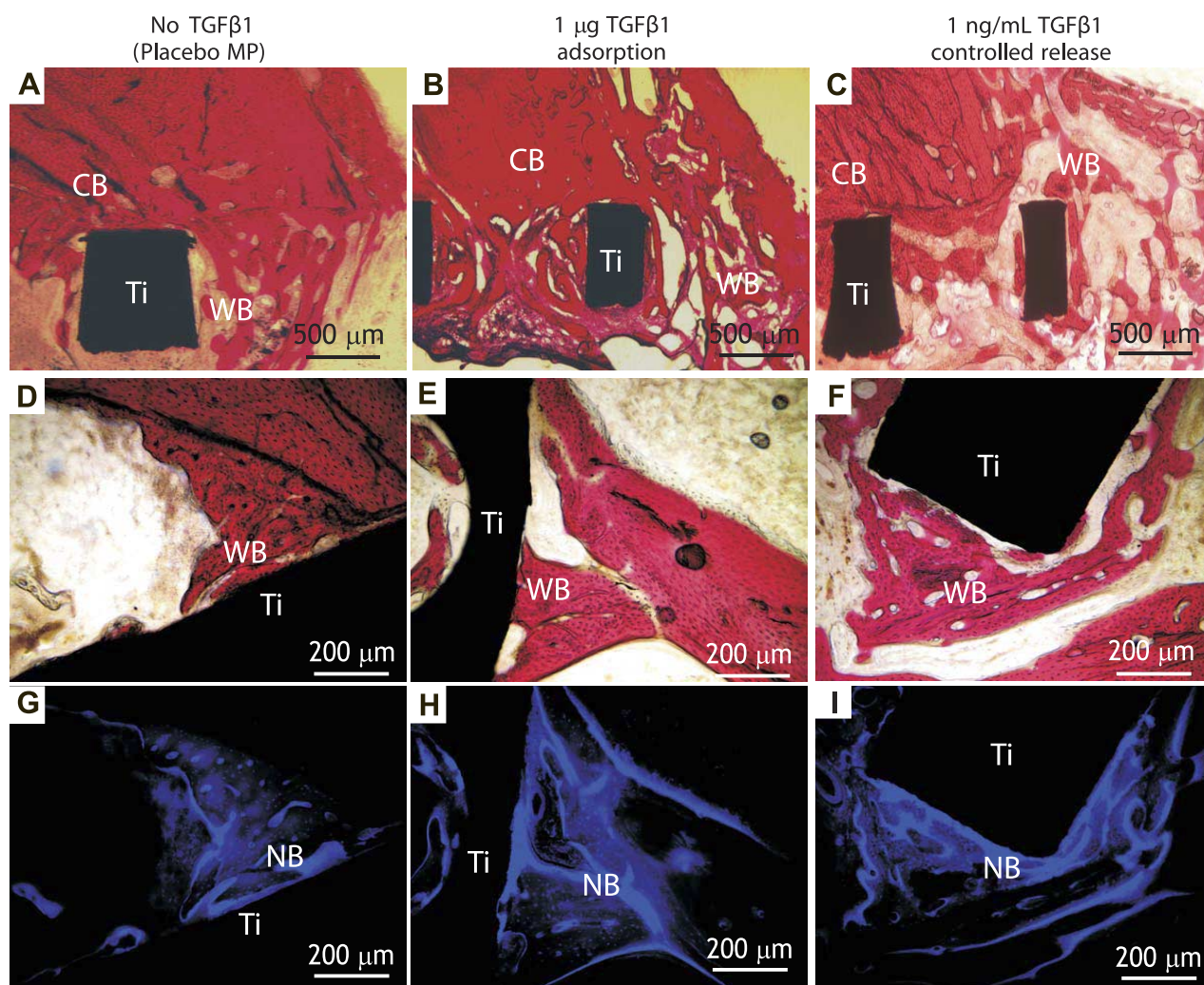

Figure 4. Areas of periprosthetic new bone formation in relation to cortical bone and marrow cavity. Woven bone (WB) surrounding the porous Ti implant was substantial and integrated to cortical bone (CB) for both 1-μg gelatin-adsorbed TGF-β1 implant (*B*) and 100-ng MP-encapsulated TGF-β1 implant (*C*), in contrast to TGF-β1-free or placebo MP implant (*A*). Newly formed WB is surrounded by bone marrow cavity (*D–F*), which is known as a source of mesenchymal stem cells, osteoprogenitor cells, and osteoblasts, among other cell lineages. Calcein labeling revealed marked new bone (NB) formation next to the Ti implants for both 1 μg gelatin-adsorbed TGF-β1 (h) or 1 ng/ml control-released TGF-β1 (*I*), in comparison to moderate NB formation adjacent to the TGF-β1-free implant (*G*). H&E staining (A–F).

TGF-β1 implant (**Fig. 5B**) and 1 ng/ml control-released TGF-β1 implant (Fig. 5C), in comparison with the TGF-β1-free or placebo MP implant (Fig. 5A). μCT revealed marked bone ingrowth into the pores of Ti implants for both 1-μg gelatin-adsorbed TGF-β1 (Fig. 5E) and 1 ng/ml microencapsulated TGF-β1 (Fig. 5F), in comparison with the TGF-β1-free or placebo MP implant (Fig. 5D). BIC and BV/TV within the implant's pores were quantified using computerized histomorphometry, per our previous methods (28, 31). Both BIC and BV/TV for control-released 1 ng/ml TGF-β1 were significantly higher ($46 \pm 16\%$ and $29 \pm 9.6\%$, respectively) than placebo MPs ($24 \pm 8\%$ and $19 \pm 6.2\%$, respectively) ($P < 0.05$, $n=6$) (Fig. 5G), representing 96% increase in BIC and 50% increase in BV/TV. Importantly, the BIC and BV/TV yielded by 1 ng/ml control-released TGF-β1 showed no significant differences from 1 μg gelatin-adsorbed TGF-β1 (BIC: $49 \pm 19\%$, BV/TV: $31 \pm 11\%$) ($P < 0.01$, $n=6$) (Fig. 5G),

again suggesting that controlled release is effective at a 10-fold less drug dose than adsorption.

DISCUSSION

For the replacement of diseased or missing tissues and organs, synthetic implants are advantageous because of a lack of donor site morbidity, virtually endless supply, and the potential for packaged delivery in the operating room. In contrast to the premise of current solid and inert prosthesis design, the present approach shows that porous implants serve as delivery framework for controlled release of microencapsulated bioactive cues. The present observation of increased bone-to-implant contact by 96% and bone ingrowth by 50% *via* control-released TGF-β1 over placebo MPs is comparable to a number of reported *in vivo* studies of the efficacy of bone ingrowth by growth factor adsorption
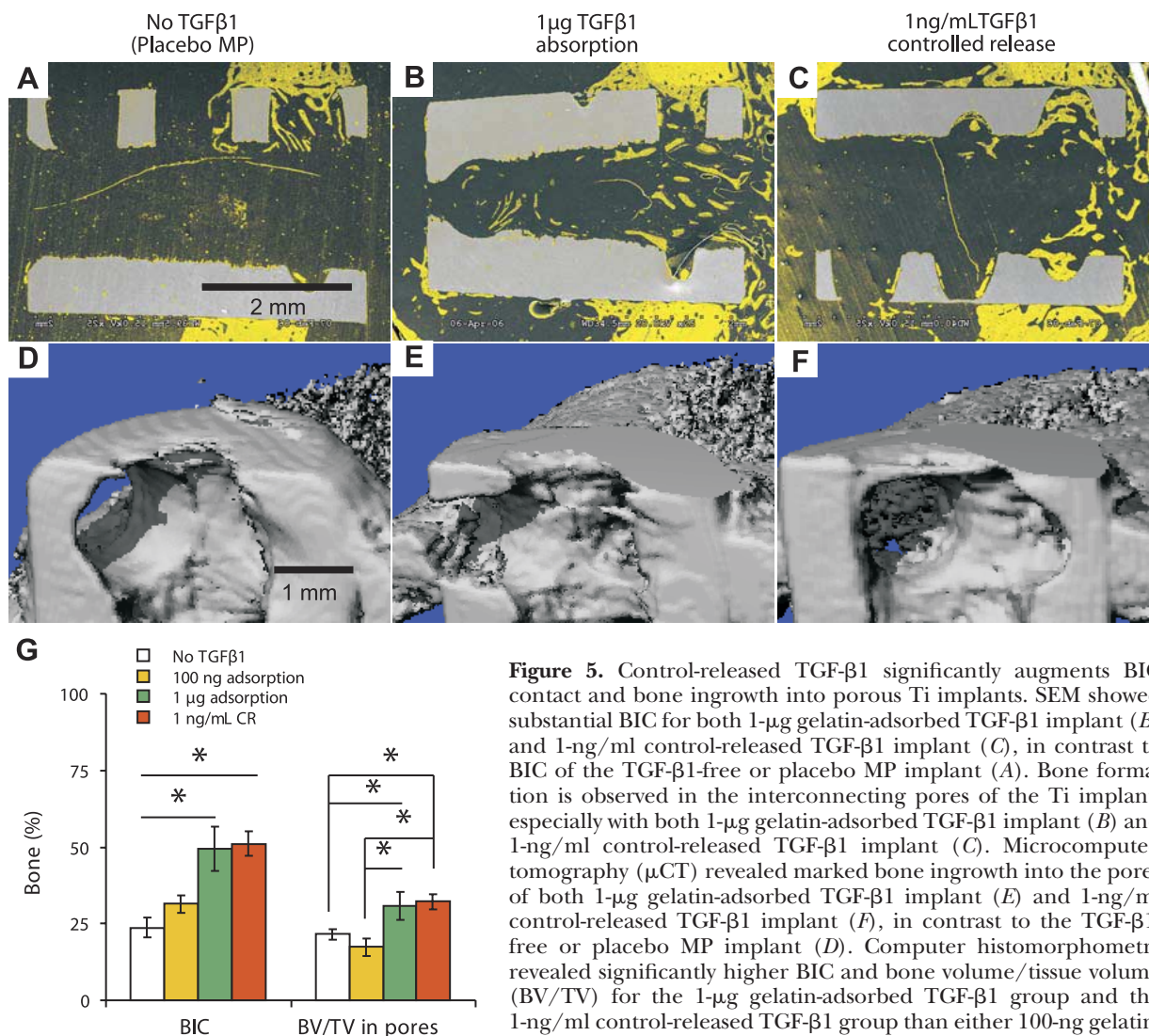

Figure 5. Control-released TGF-β1 significantly augments BIC contact and bone ingrowth into porous Ti implants. SEM showed substantial BIC for both 1-μg gelatin-adsorbed TGF-β1 implant (*B*) and 1-ng/ml control-released TGF-β1 implant (*C*), in contrast to BIC of the TGF-β1-free or placebo MP implant (*A*). Bone formation is observed in the interconnecting pores of the Ti implant, especially with both 1-μg gelatin-adsorbed TGF-β1 implant (*B*) and 1-ng/ml control-released TGF-β1 implant (*C*). Microcomputed tomography (μCT) revealed marked bone ingrowth into the pores of both 1-μg gelatin-adsorbed TGF-β1 implant (*E*) and 1-ng/ml control-released TGF-β1 implant (*F*), in contrast to the TGF-β1-free or placebo MP implant (*D*). Computer histomorphometry revealed significantly higher BIC and bone volume/tissue volume (BV/TV) for the 1-μg gelatin-adsorbed TGF-β1 group and the 1-ng/ml control-released TGF-β1 group than either 100-ng gelatin-adsorbed TGF-β1 or TGF-β1-free or placebo MP group (*G*) (*n*=6; *$P < 0.05$). There are no statistically significant differences in either BIC or BV/TV between the 1-μg gelatin-adsorbed TGF-β1 group and the 1-ng/ml control-released TGF-β1 group, suggesting that controlled release is effective at a 10-fold less drug dose than adsorption (see text for 1-ng/ml dose conversion to 100-ng drug dose).

in biomaterials that coat implant surface (28, 31), but with the important difference that the present controlled-release approach reduces drug dose by 10-fold. This 10-fold decrease in drug dose may have significant implications in potential reductions of cost and toxicity of *in vivo* delivered biological cues. Our findings further provide strong evidence that control-released TGF-β1 *via* porous Ti implants not only induces the migration and proliferation of hMSC *in vitro*, but also enhances bone ingrowth and bone-to-implant contact *in vivo*. Thus, the excessive mass of solid implants can be made porous as a drug delivery carrier for controlled-release of microencapsulated bioactive cues. Porous implant design also increases the surface area for cell adhesion and bone ingrowth. New bone growing into the interconnecting pores of porous implants, as shown in the present study, may provide bone interlocking, further enhancing bone ingrowth and long-term peri-prosthetic bone health.

Although we used TGF-β1 as a bioactive cue, the present system is versatile and can incorporate any bioactive cues, such as bone morphogenetic proteins (BMPs) (13, 33). TGF-β1 and BMP2 are both efficacious in enhancing implant bone ingrowth (15, 17, 28). TGF-β1 stimulates the production of fibronectin, collagen, integrin, and proteoglycans (34–36). TGF-β1 is selected in the present work primarily due to our immediate goal to enhance the initial phase of cell chemotaxis and proliferation in implant wound healing. In general, the delivery of bioactive cues for synthetic implants has been accomplished by two approaches, adsorption directly on implant surface or adsorption in biomaterials that coat implant surface (37). Previous reports of the adsorption of growth factors usually rely on large doses in animal models, likely presenting as obstacles when translated to human patients due to potential side effects, denature and diffusion of growth factors, and high cost (37). Proteins and peptides exposed to the *in vivo* environment, rich in enzymes and catalysts, are known to undergo diffusion and denature, and may fail to achieve the intended effects. Diffusion and/or denature of bioactive cues prior to the binding to their receptors likely account for the ineffectiveness of the presently delivered low-dose 100 ng TGF-β1 by adsorption. In contrast, control-released TGF-β1 at the same dose, 100 ng, significantly augments bone ingrowth. Although a higher dose of adsorbed 1 μg gelatin-adsorbed TGF-β1 was as effective as 100 ng control-released TGF-β1, the proportionally high dose in association with adsorption in patients may present as problems such as toxicity, high cost, and regulatory difficulties. In general, there is likely a discrepancy between *in vitro* and *in vivo* release profiles. It is remarkably difficult to study *in vivo* release profiles, given the complexity of the biological system that is vascularized and filled with endogenous cytokines. Nonetheless, like other *in vivo* release systems, the effect of *in vivo* regeneration is a meaningful parameter for the effectiveness, or the lack, of the *in vivo* release system. In this case, *in vivo* release of TGF-β1 yielded 96% greater BIC and 50% greater BV/TV, indicating its effectiveness.

Because dental and orthopedic implants are in contact with bone marrow, the role played by bone marrow cells, including multipotent stem cells (38, 39), warrants investigation in implant bone healing (38, 39). However, previous implant studies examined the participation of osteoblasts in implant wound healing, but rarely MSC (12, 13, 26, 28, 40). The presently observed chemotaxis, proliferation, and differentiation of MSC *in vitro* may translate to increased numbers of not only MSC, but also other cells, such as osteoprogenitors in an osteogenic environment. Thus, the augmentation of bone ingrowth in the surface and pores of Ti implants *in vivo* is likely contributed by the modulation of the chemotaxis and proliferation of osteoprogenitor cells, including MSC by control-released TGF-β1. Although TGF-β1 may conceptually have attracted cell lineages other than MSC or osteoblasts, our observed integration of the rabbit humerus implants, stability on harvest, and peri-implant bone formation provides evidence against the sum effects of overwhelming attachment of, for example, fibroblasts, to implant surface. Besides orthopedic and dental prostheses, other applications of porous implants may include spinal cages, coronary implants, maxillofacial implants, or any solid prostheses in current use but without the delivery of bioactive cues, especially by controlled release. We speculate that control-released bioactive cues are able to home tissue-forming cells into the implant's interconnecting pores, and induce tissue formation from inside out, in addition to the outside-in tissue integration on implant surface. This postulate can be tested by delivering labeled cells in porous implants. Nonetheless, the present approach relies on the homing of host cells that are involved in implant bone healing, offering an attractive modality for translation. Taken together, the present findings provide the proof of concept for testing the potential augmentation of bone ingrowth in porous implants by controlled release of bioactive cues in large animal models and potentially patients. Potential transformation of inert and solid synthetic implants into a porous, bioactive drug delivery system may accelerate tissue integration in the restoration of the function of diseased or missing tissues and organs. [FJ]

REFERENCES

1. Misch, C. E. (1993) *Contemporary Implant Dentistry*, Mosby, Chicago
2. Albrektsson, T., Branemark, P. I., Hansson, H. A., and Lindstrom, J. (1981) Osseointegrated titanium implants. Require-

ments for ensuring a long-lasting, direct bone-to-implant anchorage in man. *Acta Orthop. Scand.* **52,** 155–170

3. An, Y. H. (2000) Mechanical properties of bone. In *Mechanical Testing of Bone and the Bone-implant Interface* (An, Y. H., and Draughn, R. A., eds) pp. 41–63, CRC Press, New York

4. Ratner, B. D., Hoffman, A. S., Schoen, F. J., and Lemons, J. E. (1996) *Biomaterials Science: An Introduction to Materials in Medicine,* Academic Press, New York

5. McCarthy, E. F., and Frassica, F. J. (1998) *Pathology of Bone and Joint Disorders,* W.B. Saunders Company, Philadelphia

6. McKoy, B. E., An, Y. H., and Friedman, R. J. (2000) Factors affecting the strength of the bone-implant interface. In *Mechanical Testing of Bone and the Bone-implant Interface* (An, Y. H., and Draughn, R. A., eds) pp. 439–462, CRC Press, New York

7. Ingham, E., and Fisher, J. (2000) Biological reactions to wear debris in total joint replacement. *Proc. Inst. Mech. Eng. [H]* **214,** 21–37

8. Lossdorfer, S., Schwartz, Z., Wang, L., Lohmann, C. H., Turner, J. D., Wieland, M., Cochran, D. L., and Boyan, B. D. (2004) Microrough implant surface topographies increase osteogenesis by reducing osteoclast formation and activity. *J. Biomed. Mater. Res. A* **70,** 361–369

9. Meredith, D. O., Riehle, M. O., Curtis, A. S., and Richards, R. G. (2007) Is surface chemical composition important for orthopaedic implant materials? *J. Mater. Sci. Mater. Med.* **18,** 405–413

10. Nebe, J. G., Luethen, F., Lange, R., and Beck, U. (2007) Interface interactions of osteoblasts with structured titanium and the correlation between physicochemical characteristics and cell biological parameters. *Macromol. Biosci.* **7,** 567–578

11. Roberts, A. B. (2000) Transforming growth factor-beta In *Skeletal Growth Factors* (Canalis, E., ed) pp. 233–249, Lippincott, Williams, and Wilkins, Philadelphia

12. Alliston, T. N., and Derynck, R. (2000) Transforming growth factor-β in skeletal development and maintenance. In *Skeletal Growth Factors* (Canalis, E., ed) pp. 233–249, Lippincott, Williams, and Wilkins, Philadelphia

13. Dimitriou, R., Tsiridis, E., and Giannoudis, P. V. (2005) Current concepts of molecular aspects of bone healing. *Injury* **36,** 1392–1404

14. Zhang, H., Aronow, M. S., and Gronowicz, G. A. (2005) Transforming growth factor-beta 1 (TGF-β1) prevents the age-dependent decrease in bone formation in human osteoblast/implant cultures. *J. Biomed. Mater. Res. A* **75,** 98–105

15. Liu, Y., Enggist, L., Kuffer, A. F., Buser, D., and Hunziker, E. B. (2007) The influence of BMP-2 and its mode of delivery on the osteoconductivity of implant surfaces during the early phase of osseointegration. *Biomaterials* **28,** 2677–2686

16. Sumner, D. R., Turner, T. M., Urban, R. M., Virdi, A. S., and Inoue, N. (2006) Additive enhancement of implant fixation following combined treatment with rhTGF-β2 and rhBMP-2 in a canine model. *J. Bone. Joint. Surg. Am.* **88,** 806–817

17. Zhang, R., An, Y., Toth, C. A., Draughn, R. A., Dimaano, N. M., and Hawkins, M. V. (2004) Osteogenic protein-1 enhances osseointegration of titanium implants coated with peri-apatite in rabbit femoral defect. *J. Biomed. Mater. Res. B. Appl. Biomater.* **71,** 408–413

18. Holland, T. A., Bodde, E. W., Cuijpers, V. M., Baggett, L. S., Tabata, Y., Mikos, A. G., and Jansen, J. A. (2007) Degradable hydrogel scaffolds for in vivo delivery of single and dual growth factors in cartilage repair. *Osteoarthritis Cartilage* **15,** 187–197

19. Moioli, E. K., Hong, L., Guardado, J., Clark, P. A., and Mao, J. J. (2006) Sustained release of TGF-β3 from PLGA microspheres and its effect on early osteogenic differentiation of human mesenchymal stem cells. *Tissue Eng.* **12,** 537–546

20. Moioli, E. K., Clark, P. A., Xin, X., Lal, S., and Mao, J. J. (2007) Matrices and scaffolds for drug delivery in dental, oral and craniofacial tissue engineering. *Adv. Drug. Deliv. Rev.* **59,** 308–324

21. Moioli, E. K., Hong, L., and Mao, J. J. (2007) Inhibition of osteogenic differentiation of human mesenchymal stem cells. *Wound Repair Regen.* **15,** 413–424

22. Cohen, S., Yoshioka, T., Lucarelli, M., Hwang, L. H., and Langer, R. (1991) Controlled delivery systems for proteins based on poly(lactic/glycolic acid) microspheres. *Pharm. Res.* **8,** 713–720

23. Marion, N. W., and Mao, J. J. (2006) Mesenchymal stem cells and tissue engineering. *Methods Enzymol.* **420,** 339–361

24. Hong, L., Peptan, I., Clark, P., and Mao, J. J. (2005) Ex vivo adipose tissue engineering by human marrow stromal cell seeded gelatin sponge. *Ann. Biomed. Eng.* **33,** 511–517

25. Cory, A. H., Owen, T. C., Barltrop, J. A., and Cory, J. G. (1991) Use of an aqueous soluble tetrazolium/formazan assay for cell growth assays in culture. *Cancer Commun.* **3,** 207–212

26. Yamamoto, M., Tabata, Y., Hong, L., Miyamoto, S., Hashimoto, N., and Ikada, Y. (2000) Bone regeneration by transforming growth factor β1 released from a biodegradable hydrogel. *J. Control. Release* **64,** 133–142

27. Sumner, D. R., Turner, T. M., and Urban, R. M. (2001) Animal models relevant to cementless joint replacement. *J. Musculoskelet. Neuronal Interact.* **1,** 333–345

28. Lind, M. (1998) Growth factor stimulation of bone healing. Effects on osteoblasts, osteomies, and implants fixation. *Acta Orthop. Scand. Suppl.* **283,** 2–37

29. Sumner, D. R., Turner, T. M., Urban, R. M., Leven, R. M., Hawkins, M., Nichols, E. H., McPherson, J. M., and Galante, J. O. (2001) Locally delivered rhTGF-β2 enhances bone ingrowth and bone regeneration at local and remote sites of skeletal injury. *J. Orthop. Res.* **19,** 85–94

30. Clark, P. A., Rodriguez, A., Sumner, D. R., Hussain, M. A., and Mao, J. J. (2005) Modulation of bone ingrowth of rabbit femur titanium implants by in vivo axial micromechanical loading. *J. Appl. Physiol.* **98,** 1922–1929

31. De Ranieri, A., Virdi, A. S., Kuroda, S., Shott, S., Leven, R. M., Hallab, N. J., and Sumner, D. R. (2005) Local application of rhTGF-β2 enhances peri-implant bone volume and bone-implant contact in a rat model. *Bone* **37,** 55–62

32. Alhadlaq, A., Elisseeff, J. H., Hong, L., Williams, C. G., Caplan, A. I., Sharma, B., Kopher, R. A., Tomkoria, S., Lennon, D. P., Lopez, A., and Mao, J. J. (2004) Adult stem cell driven genesis of human-shaped articular condyle. *Ann. Biomed. Eng.* **32,** 911–923

33. Linkhart, T. A., Mohan, S., and Baylink, D. J. (1996) Growth factors for bone growth and repair: IGF, TGF β and BMP. *Bone* 19:1S–12S

34. Doll, B., Sfeir, C., Winn, S., Huard, J., and Hollinger, J. (2001) Critical aspects of tissue-engineered therapy for bone regeneration. *Crit. Rev. Eukaryot. Gene. Exp.* **11,** 173–198

35. Lu, L., Stamatas, G. N., and Mikos, A. G. (2000) Controlled release of transforming growth factor beta1 from biodegradable polymer microparticles. *J. Biomed. Mater. Res.* **50,** 440–451

36. Leach, J. K., and Mooney, D. J. (2004) Bone engineering by controlled delivery of osteoinductive molecules and cells. *Expert Opin. Biol. Ther.* **4,** 1015–1027

37. Schliephake, H., Scharnweber, D., Dard, M., Sewing, A., Aref, A., and Roessler, S. (2005) Functionalization of dental implant surfaces using adhesion molecules. *J. Biomed. Mater. Res. B Appl. Biomater.* **73,** 88–96

38. Alhadlaq, A., and Mao, J. J. (2004) Mesenchymal stem cells: isolation and therapeutics. *Stem. Cells. Dev.* **13,** 436–448

39. Pittenger, M. F., Mackay, A. M., Beck, S. C., Jaiswal, R. K., Douglas, R., Mosca, J. D., Moorman, M. A., Simonetti, D. W., Craig, S., and Marshak, D. R. (1999) Multilineage potential of adult human mesenchymal stem cells. *Science* **284,** 143–147

40. Hunziker, E. B., and Rosenberg, L. C. (1996) Repair of partial-thickness defects in articular cartilage: cell recruitment from the synovial membrane. *J. Bone Joint. Surg. Am.* **78,** 721–733